Immunity, Vol. 22, 163–173, February, 2005, Copyright ©2005 by Elsevier Inc. DOI 10.1016/j.immuni.2004.12.011

Broadly Neutralizing Anti-HIV Antibody 4E10 Recognizes a Helical Conformation of a Highly Conserved Fusion-Associated Motif in gp41

Rosa M.F. Cardoso,[1] Michael B. Zwick,[2] Robyn L. Stanfield,[1] Renate Kunert,[5] James M. Binley,[4] Hermann Katinger,[5] Dennis R. Burton,[1,2,*] and Ian A. Wilson[1,3,*]

[1]Department of Molecular Biology
[2]Department of Immunology and
[3]Skaggs Institute for Chemical Biology
The Scripps Research Institute
La Jolla, California 92037
[4]Torrey Pines Institute for Molecular Studies
San Diego, California 92121
[5]Institute of Applied Microbiology
University of Agriculture
A-1190 Vienna
Austria

Summary

Broadly neutralizing monoclonal antibodies to HIV-1 are rare but invaluable for vaccine design. 4E10 is the broadest neutralizing antibody known and recognizes a contiguous and highly conserved epitope in the membrane-proximal region of gp41. The crystal structure of Fab 4E10 was determined at 2.2 Å resolution in complex with a 13-residue peptide containing the gp41 core epitope (NWFDIT). The bound peptide adopts a helical conformation in which the key contact residues, Trp^{P672}, Phe^{P673}, Ile^{P675}, and Thr^{P676}, map to one face of the helix. The peptide binds in a hydrophobic pocket that may emulate its potential interaction with the host cell membrane. The long CDR H3 of the antibody extends beyond the bound peptide in an orientation that suggests that its apex could contact the viral membrane when 4E10 is bound to its membrane-proximal epitope. These structural insights should assist in the design of immunogens to elicit 4E10-like neutralizing responses.

Introduction

The success of immunoprophylaxis in animal models using HIV-1-neutralizing monoclonal antibodies suggests that, if neutralizing antibodies could be generated by an appropriate vaccine, they would provide substantial benefit (Ferrantelli and Ruprecht, 2002; Mascola, 2003; Burton et al., 2004). However, the goal of designing immunogens that elicit neutralizing antibodies against multiple isolates of HIV-1 has been extraordinarily difficult to achieve. The vast majority of anti-HIV-1 antibodies elicited either by immunization or during natural infection have limited or no crossneutralizing activity to other HIV-1 isolates and typically bind to nonconserved epitopes or epitopes that are poorly exposed on infectious virions. Only a handful of potent and broadly crossreactive human monoclonal antibodies (mAbs) have been identified to date against HIV-1 primary isolates and include mAbs b12, 2G12, 2F5, and 4E10. These rare mAbs have been derived from HIV-1-infected patients and target conserved but distinct epitopes on gp120 or gp41, the HIV-1 envelope (Env) glycoproteins responsible for mediating HIV entry into human cells (Weissenhorn et al., 1997; Chan et al., 1997; Kwong et al., 1998; Wyatt and Sodroski, 1998; Gallo et al., 2003). mAb b12 binds to the recessed CD4 binding site on gp120 (Saphire et al., 2001), whereas mAb 2G12 recognizes a unique cluster of oligomannose sugars on the gp120 outer domain (Calarese et al., 2003). mAbs 4E10 and 2F5 recognize adjacent and highly conserved contiguous epitopes in the extreme C-terminal, membrane-proximal region of gp41 (Figure 1), indicating that gp41 is not completely masked from Ab recognition by gp120. The 2F5 epitope is centered around the sequence ELDKWA (Muster et al., 1993; Pai et al., 2000; Ofek et al., 2004), whereas 4E10 recognizes an epitope containing the sequence NWF(D/N)IT (Zwick et al., 2001b, 2005; Kunert et al., 2004) in a Trp-rich region of gp41 immediately C-terminal to the 2F5 epitope. Simultaneous targeting of multiple conserved epitopes on HIV is likely to be the best strategy for vaccine development to maximize the breadth of protection (Zwick et al., 2001b; Kitabwalla et al., 2003). As a single agent, 4E10 is the broadest HIV-1-neutralizing mAb described to date with activity against isolates from most HIV-1 clades, including A, B, C, D, E, and G, albeit sometimes with less potency than the other three more clade-restricted mAbs described above (Binley et al., 2004).

The conserved C-terminal region of the gp41 extracellular domain that encompasses the 4E10 and 2F5 epitopes is critical for Env-mediated membrane fusion and virus infectivity (Salzwedel et al., 1999; Munoz-Barroso et al., 1999). Alanine mutation of three of five highly conserved tryptophan residues (Trp^{666}, Trp^{670}, and Trp^{672}; numbered according to the HXB2 isolate sequence) in this membrane-proximal region greatly reduces viral entry (Salzwedel et al., 1999). Moreover, the induction of membrane leakage by a peptide corresponding to this Trp-rich region (Suarez et al., 2000) implies that this region may be directly involved in membrane disruption during the fusion process. However, this notion has been challenged by another mutagenesis study which suggests that the membrane-proximal region instead provides a flexible arm to gp41 to allow membrane fusion (Dimitrov et al., 2003). Overall, the conserved membrane-proximal region of gp41 appears to be highly promising for vaccine development, especially since it is the target of two (4E10 and 2F5) of the four most broadly neutralizing anti-HIV mAbs.

The three-dimensional structure of the Trp-rich membrane-proximal region of gp41 was previously investigated by NMR spectroscopy using a synthetic peptide (KWASLWNWFNITNWLWYIK) (Schibli et al., 2001). In dodecylphosphocholine micelles, the Trp-rich region has a helical structure with the Trp residues forming a "collar" around the helix axis, parallel to the water-dodecylphosphocholine interface of the micelle. How-

*Correspondence: burton@scripps.edu (D.R.B.); wilson@scripps.edu (I.A.W.)

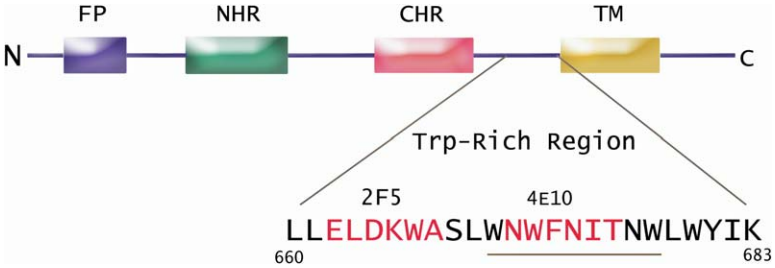

Figure 1. Schematic Representation of gp41

Important functional regions include the fusion peptide (FP, purple box), the N- and C-terminal heptad repeat regions (NHR, green box, and CHR, red box, respectively), and the transmembrane region (TM, yellow box). The location and sequence of the Trp-rich region are indicated with the core 2F5 and 4E10 epitopes shown in red, and the sequence contained within the peptide used in this study is underlined. Sequence numbering follows strain HXB2. The various domains are not drawn to scale.

ever, the precise orientation of this region in the natural context of the native gp120-gp41 trimer and how it might rearrange during the fusion process remain unknown. To examine the interaction of 4E10 with its epitope on gp41 at the atomic level, we determined the crystal structure of Fab 4E10 in complex with a soluble synthetic 13-residue peptide (KGWNWFDITNWGK) (Zwick et al., 2001a) that encompasses the 4E10 epitope and corresponds to the W670-W678 consensus group M sequence of gp160. The structure of this complex reveals the epitope conformation recognized by 4E10 and its interaction with this broadly neutralizing antibody.

Results

Structure Determination of a Fab 4E10-Peptide Complex

To examine the interaction of 4E10 with the Trp-rich membrane-proximal region of gp41, the crystal structure of a Fab 4E10-peptide epitope complex was determined at 2.2 Å resolution. The 4E10 epitope is contained within the 13-residue peptide (Lys^{P668} Gly^{P669} Trp^{P670} Asn^{P671} Trp^{P672} Phe^{P673} Asp^{P674} Ile^{P675} Thr^{P676} Asn^{P677} Trp^{P678} Gly^{P679} Lys^{P680}; numbered according to the HXB2 isolate sequence with a P chain identifier) that was previously shown to bind 4E10 (in that study, the peptide was named KGND) (Zwick et al., 2001a). The Lys and Gly residues at either end of this peptide were added to increase peptide solubility in water.

Human IgG3 4E10 was originally isolated from a clade B HIV-1-positive individual (Buchacher et al., 1994). Fab 4E10 was obtained by papain digestion of the recombinant IgG1(κ) 4E10, produced in Chinese hamster ovary (CHO) cells (Kunert et al., 2004). The complex of Fab 4E10 and peptide was achieved by overnight incubation of the Fab at 4°C with a five times molar excess of peptide. Crystals grew after about one week as clusters of thin plates, which were carefully separated into individual plates for X-ray data collection. The data were indexed in space group C2 with two 4E10-peptide complexes per asymmetric unit (61.5% solvent content and Matthews' coefficient of 3.2 $Å^3$ Da^{-1}). The structure was determined by molecular replacement using Fab 48G7, a catalytic antibody (Protein Data Bank [PDB] entry 1HKL), as the initial model and was then refined to a resolution of 2.2 Å with R_{cryst} = 21.7%, and R_{free} = 26.0% (Table 1). The final model contains Fab residues L1-L212, H1-H232 (Fab residues are numbered according to standard convention [Kabat et al., 1991] with light and heavy chain identifiers L and H, respectively) and peptide residues P669–P680. Heavy-chain C-terminal residues (Ser^{H229}, Cys^{H230}, Asp^{H231}, and Lys^{H232}) were visible in one Fab (molecule 1). Electron density omit maps clearly defined the location and conformation of the peptide in the 4E10 binding site (Figure 2A). The only peptide residue which had no interpretable electron density was the N-terminal Lys^{P668}, which was not included in the model.

The Fab 4E10-peptide complex model has good geometry with only Ala^{L51}, which is in a highly conserved γ turn as in most antibody structures (Stanfield et al., 1999), in the disallowed region of the Ramachandran plot (Table 1). As expected, the two molecules in the asymmetric unit are similar, with rms deviations (Cα) less than 0.4 Å. Only the complex with lower B values (molecule 1) will be described here.

The Structure of Fab 4E10

Fab 4E10 has the canonical β sandwich immunoglobulin fold with an elbow angle of 193° in both independent antibody molecules. The complementarity determining regions (CDRs) or hypervariable loops L1, L2, L3, H1, and H2 belong to canonical classes 2, 1, 1, 1, and 2, respectively, as determined from the length, sequence, and conformation of the loops (Al-Lazikani et al., 1997) (Figures 3A and 3B). CDR H3 bends away from the binding site to allow interaction of its base and central residues with the C-terminal region of the peptide (Figure 3B).

Antibody 4E10 has a long CDR H3 (Glu^{H95} Gly^{H96} Thr^{H97} Thr^{H98} Gly^{H99} Trp^{H100} Gly^{H100A} Trp^{H100B} Leu^{H100C} Gly^{H100D} Lys^{H100E} Pro^{H100F} Ile^{H100G} Gly^{H100H} Ala^{H100I} Phe^{H100J} Ala^{H101} His^{H102}) with a ten amino acid insert after residue 100. Such long CDR H3 loops are also found in other HIV-1 mAbs, such as 2F5 (Pai et al., 2000; Ofek et al., 2004), Z13 (Zwick et al., 2001a), b12 (Saphire et al., 2001), 447-52D (Stanfield et al., 2004), and 17b (Kwong et al., 1998) and may facilitate access to concave or relatively inaccessible sites. In addition, the tip of the H3 loop of 4E10 is composed of mainly nonpolar residues (Gly^{H99}, Trp^{H100}, Gly^{H100A}, Trp^{H100B}, Leu^{H100C}, and Gly^{H100D}) (Figure 3C) that form a quite hydrophobic surface. As only two of these residues (Leu^{H100C} and Gly^{H100D}; Table 2) contact the peptide epitope, the other hydrophobic residues are positioned such that they could interact with the adjacent viral membrane and/or other residues of gp41. The five Gly residues may provide the loop with the appropriate conformational flexi-

Table 1. X-Ray Diffraction Data and Refinement Statistics for the 4E10-Peptide Complex

Crystal Features	
Space group	C2
No. of molecules of complex per asymmetric unit	2
Unit cell parameters (Å, °)	a = 157.3, b = 45.1, c = 198.5, β = 113.8
Data Quality	
Resolution (Å)[a]	50.00–2.20 (2.28–2.20)
No. of observations	198,794
No. of unique reflections	61,572
Mosaicity (°)	0.35
Completeness (%)[a]	93.0 (61.4)
Multiplicity[a]	3.2 (2.2)
I/σ(I)[a]	16.7 (2.3)
R_{sym} (%)[a,b]	7.5 (37.1)
Model Quality	
R_{cryst} (%)[c]	21.7
R_{free} (%)[c]	26.0
No. of protein atoms	6907
No. of water molecules	612
Average B value (Å^2)	
Molecule 1 (heavy, light, peptide)	22.2, 19.5, 28.3
Molecule 2 (heavy, light, peptide)	41.0, 46.5, 33.8
Water molecules	36.2
Rms deviation for bond lengths (Å)	0.005
Rms deviation for bond angles (°)	1.3
Ramachandran plot	
Most favored regions (%)	87.2
Additional allowed regions (%)	12.4
Generously allowed regions (%)	0.1
Disallowed regions (%)	0.3[d]

[a] Values in parentheses correspond to the highest resolution shell.
[b] $R_{sym} = [\Sigma_h\Sigma_i|I_i(h) - <I(h)>|/\Sigma_h\Sigma_i I_i(h)] \times 100$, where <I(h)> is the mean of the I(h) observation of reflection i.
[c] $R = \Sigma_{hkl}|F_o - F_c|/\Sigma_{hkl}|F_o|$. R_{free} was calculated as R but using only 5% of data reserved for the crossvalidation.
[d] The only residue present in the disallowed region is Ala^{L51}, which is in a conserved γ turn, as observed in most antibody structures (Stanfield et al., 1999).

bility, while the Trp residues may facilitate interactions with hydrophobic regions in or around the membrane-proximal region of gp41, including the viral membrane. This remarkably hydrophobic flat tip resembles the structure described for the H3 loop of 2F5 (Ofek et al., 2004), another HIV-1-neutralizing antibody that also binds to the membrane-proximal region of gp41.

Another noteworthy characteristic of 4E10 is the remarkable hydrophobicity of its combining site (Figure 3D), which is derived in part from the H3 loop as well as from an unusually hydrophobic H2 loop (Gly^{H50} Val^{H51} Ile^{H52} Pro^{H52A} Leu^{H53} Leu^{H54} Thr^{H55} Ile^{H56} Thr^{H57} Asn^{H58} Tyr^{H59} Ala^{H60}). Nevertheless, the amino acid composition, particularly of L1, L3, and part of H3, contributes sufficient hydrophilic interactions to stabilize the otherwise exposed binding site.

The Structure of the 4E10 Epitope

The 13-residue peptide is bound to Fab 4E10 in a helical conformation (Figures 2–4), as found for a 19-residue peptide corresponding to the Trp-rich membrane-proximal region of gp41 in membrane-mimetic dodecylphosphocholine micelles by NMR spectroscopy (Schibli et al., 2001). The 13-residue peptide has an α-helical conformation from Asp^{P674} to Lys^{P680} preceded by a short 3_{10} helix (Asn^{P671} and Trp^{P672}) and an extended structure (Gly^{P669} and Trp^{P670}) at the N terminus (Figures 2B and 2C). The transition from 3_{10} helix to α helix occurs at Phe^{P673}, where its carbonyl oxygen makes a water-mediated hydrogen bond to the backbone nitrogen of Asn^{P677} (Figure 2B), the i+4 residue from Phe^{P673}, in an almost α-helical manner. The 3_{10} helix has been suggested to act as a folding intermediate in α-helix formation. The helical conformation creates an amphipathic structure with a narrow polar face (defined by Asn^{P671}, Asp^{P674}, Asn^{P677}, and Lys^{P680}) and a large hydrophobic face (Trp^{P672}, Phe^{P673}, Ile^{P675}, Thr^{P676}, Trp^{P678}, and Gly^{P679}) (Figures 2C and 2D). Residue Lys^{P680}, which is part of a solubility tag, corresponds in position to the universally conserved Trp^{680} in the gp41 sequence and is located between these two faces.

In complexes between peptides and antibodies, β-turns are the predominant secondary structure of the bound peptide (Stanfield and Wilson, 1995). Thus, the helical conformation of the peptide bound to 4E10 is highly unusual. To date, only two other examples of crystal structures of complexes between helical peptides and antibodies have been deposited in the Protein Data Bank (PDB): an anti-interleukin 2 Fab in complex with an antigenic nonapeptide with seven residues in an α-helical conformation (PDB ID code 1F90) (Afonin et al., 2001) and antibody C21 in complex with its epitope on P-glycoprotein, where all 11 peptide residues form an α helix (PDB ID code 2AP2) (van den Elsen et al.,

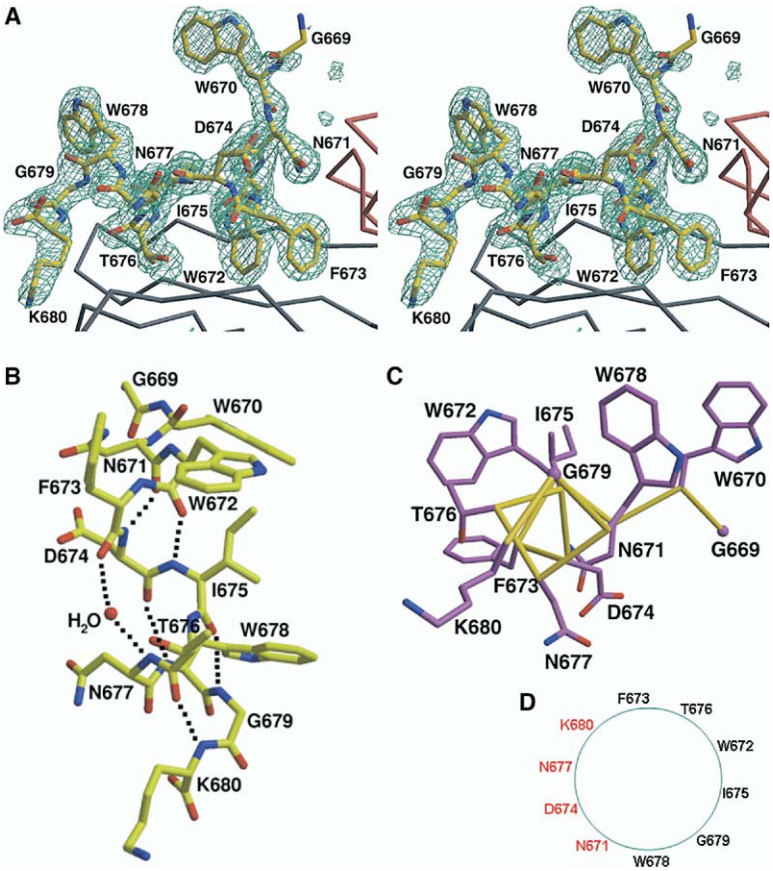

Figure 2. Structure of the Peptide Bound to Fab 4E10

The peptide sequence is KGWNWFDITNWGK and encompasses the 4E10 epitope.

(A) Stereo view of the peptide structure superimposed on the σ_A-weighted $F_o - F_c$ electron density omit map contoured at 4σ. Clear density is evident for all peptide residues, except for the two added residues at the N terminus. Part of the heavy (gray) and light (pink) chains of the antibody are displayed.

(B and C) Side (B) and top view (C) of the peptide helix. Hydrogen bonds involved in stabilization of the helical conformation are shown as dotted lines.

(D) Representation of the peptide helical wheel. The residues on the polar face are in red, and the hydrophobic face is black.

1999). Thus, this helical conformation is expected to mimic its cognate structure in gp41, particularly as 4E10 binds to and neutralizes HIV-1.

Antibody 4E10 binds with approximately 4-fold higher affinity to soluble recombinant gp41 than to the synthetic peptide (data not shown), as determined by enzyme-linked immunosorbent assays (ELISA). The reduced affinity of 4E10 for the peptide is likely due to lack of appropriate flanking residues, such as Trp^{P680} or perhaps other more distal regions of gp41, or to the inherent flexibility of the short, linear peptide. Nevertheless, the key contact residues between 4E10 and the peptide are likely to be the same as those with the core epitope on gp41.

Structural Basis for 4E10 Specificity

Specific antibody-antigen recognition comes from steric and chemical complementarity between antigen and antibody. The Fab 4E10 combining site is a largely hydrophobic cavity (Figure 3D) that allows close fit of the amphipathic peptide. The antibody surface area buried by the peptide is approximately 580 Å^2, whereas the corresponding area on the peptide is about 529 Å^2. Although these values are comparable to those found in other Fab-peptide complexes (Stanfield and Wilson, 1995), the 4E10 peptide additionally buries an extra 360 Å^2 of its surface due to crystal packing. In the crystal, the two peptide molecules are adjacent to each other and related by a two-fold crystallographic symmetry axis (Figures 3E and 3F). This supersecondary interaction of the two peptide chains (Figure 3F) combines with the antibody interaction to almost completely bury the largely hydrophobic peptide and perhaps mimics a low-energy conformation in the intact gp41 oligomer or through association with the viral membrane.

Fab 4E10 uses five of its six CDR loops to bind the peptide; CDR L2 is not used and CDR L1 makes only minor contacts (Figure 3B). Eight hydrogen bonds, one salt bridge, and 98 van der Waals contacts are made between peptide and Fab residues from CDRs L1 (4% of total contacts), L3 (28%), H1 (8%), H2 (41%), and H3 (19%) (Table 2). Ten additional hydrogen bonds between peptide and Fab residues are mediated by water molecules buried at the Fab-peptide interface.

The extent and nature of the Fab-peptide interactions define the relative importance of each peptide residue for complex formation. In a helical conformation, the peptide backbone cannot easily engage in hydrogen bonding to the Fab because of the intrapeptide hydrogen bonding along the helix. The peptide recognition then depends mainly on interactions in which the peptide side-chain knobs from the helix intercalate into holes on the antibody surface. The helical conformation of the bound peptide places the side chains of Trp^{P672} and Phe^{P673} on the same side of the peptide, and these residues, along with Ile^{P675}, Thr^{P676}, and Lys^{P680}, form an extensive hydrophobic face that intimately contacts the Fab (Figure 4). The side chains of Trp^{P672} and

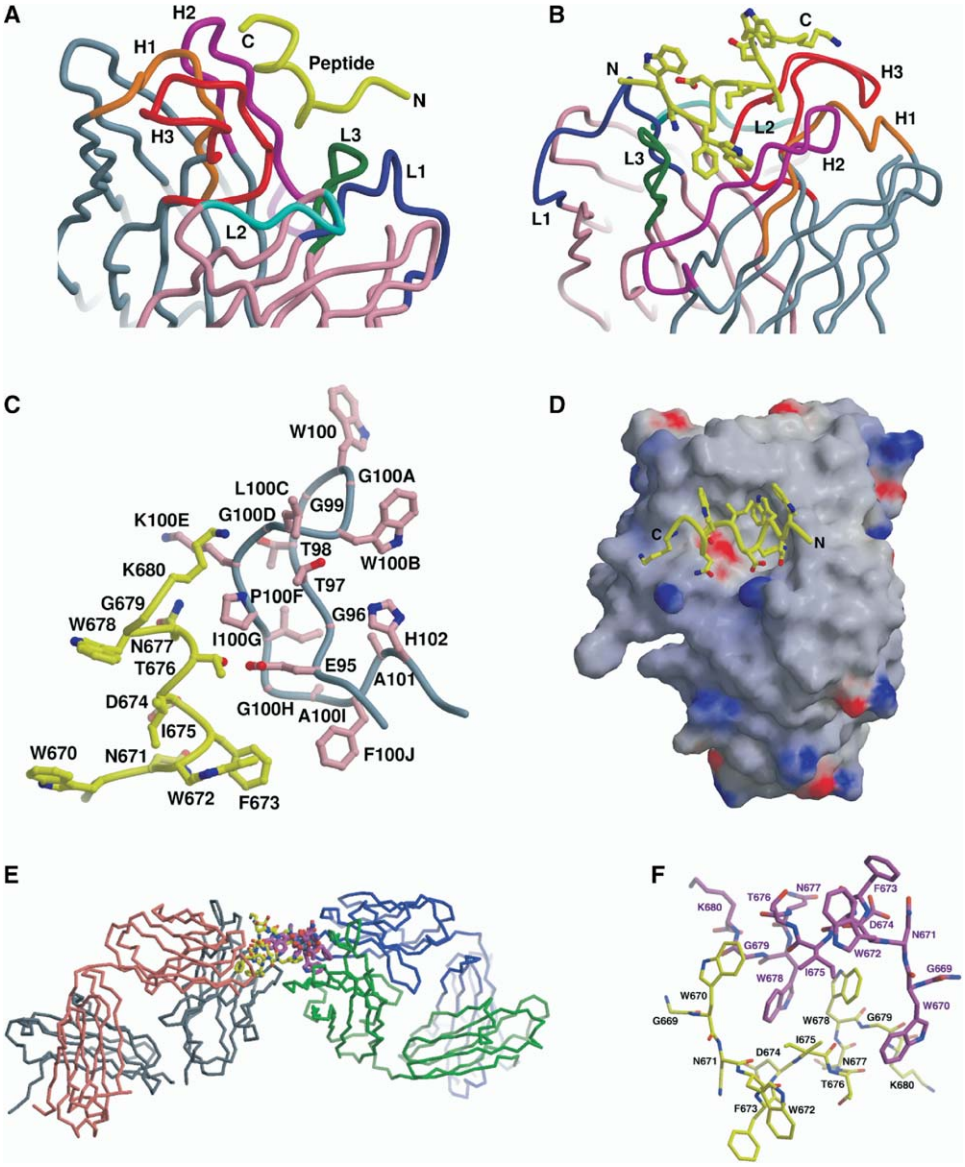

Figure 3. The Antigen Binding Site of Fab 4E10

(A and B) The CDRs L1, L2, L3, H1, H2, and H3 are highlighted in the Fab 4E10-peptide complex. The light chain (pink) with CDRs L1 (dark blue) and L3 (green) and the heavy chain (gray) CDRs H1 (orange), H2 (magenta), and H3 (red) contact the peptide (yellow). CDR L2 (cyan) does not contact antigen.

(C) Conformation of the H3 loop in the peptide-bound structure of Fab 4E10. The H3 loop (gray backbone with pink side chains) is rich in Gly and Trp residues. The bound peptide (yellow) in the complex structure is shown for reference.

(D) Electrostatic potential surface of Fab 4E10 with bound peptide. Negatively charged regions are red, positively charged regions are blue, and neutral regions are white (±15 kV potential range). The peptide (yellow) binds in a shallow hydrophobic cavity on the antibody.

(E) Overall view of two Fab 4E10-peptide complexes in the crystal unit cell. The crystal contacts in this region are close to the antigen binding site of Fab 4E10 (heavy chains are gray and green; light chains are salmon and blue). The peptides (yellow and purple chains) are located in the interface between the two related Fab molecules.

(F) Interaction of two peptide chains in the unit cell show the close interdigitation of their indole side chains, which may reflect a biologically important interaction of the peptide Trp residues with the viral membrane.

Phe^{P673} insert into a pocket in the antibody-combining site, where they form a cluster of aromatic rings with Fab residues Tyr^{L91}, Trp^{H47}, and Phe^{H100J} (Figures 4A and 4B). In addition to the 37 van der Waals contacts, the main chain and side chain of Trp^{P672} hydrogen bond to Ser^{L94} and Ile^{H56}, respectively (Table 2 and Figures 4A and 4B). The Trp^{P672} contacts represent 36% of the total contacts between Fab 4E10 and peptide (Table 2), making it the most important residue in the antibody-peptide interaction; the majority of these contacts (85%) are with CDR H2 (residues Gly^{H50}, Val^{H51}, Ile^{H52}, Ile^{H56}, and Asn^{H58}). The next key peptide residues are Thr^{P676} and Phe^{P673}, which make 18% and 14% of the total contacts with the Fab, respectively. Phe^{P673} works

Table 2. Direct Contacts between Fab 4E10 and Peptide

van der Waals Contacts	
Peptide Residue	Fab 4E10 Residue
Asn^{P671}	Gly^{L92}, Gln^{L93}, Ser^{L94}
Trp^{P672}	Ser^{L94}, Ala^{H33}, Gly^{H50}, Val^{H51}, Ile^{H52}, Ile^{H56}, Asn^{H58}
Phe^{P673}	Tyr^{L91}, Ser^{L94}, Trp^{H47}, Phe^{H100J}
Asp^{P674}	Lys^{L32}
Ile^{P675}	Ile^{H52}, Ile^{H56}
Thr^{P676}	Thr^{H31}, Tyr^{H32}, Ala^{H33}, Ile^{H52}, Glu^{H95}, Pro^{H100F}
Asn^{P677}	Pro^{H100F}
Lys^{P680}	Leu^{H100C}, Gly^{H100D}, Pro^{H100F}

Hydrogen Bond and Salt Bridge Contacts		
Peptide Atom	Fab 4E10 Atom	Distance (Å)
Trp^{P670}–O	Ser^{L94}–O_γ	3.4
Asn^{P671}–$O_{\delta1}$	Tyr^{L91}–O	2.9
Asn^{P671}–$N_{\delta2}$	Ser^{L94}–N	3.2
Trp^{P672}–N	Ser^{L94}–O_γ	3.2
Trp^{P672}–$N_{\epsilon1}$	Ile^{H56}–O	3.2
Asp^{P674}–$O_{\delta1}$	Lys^{L32}–N_ξ	3.4
Thr^{P676}–$O_{\gamma1}$	Glu^{H95}–$O_{\epsilon1}$	3.0
Thr^{P676}–$O_{\gamma1}$	Glu^{H95}–$O_{\epsilon2}$	2.8
Lys^{P680}–N_ξ	Leu^{H100C}–O	2.7

cooperatively with Trp^{P672} to form the cluster of aromatic rings in the binding site (Figure 4B). In addition to several van der Waals contacts, the hydroxyl side chain of Thr^{P676} hydrogen bonds to the carboxyl side chain of Glu^{H95} (Table 2 and Figures 4A and 4C). Thr^{P676} along with Lys^{P680} are the peptide residues with the most interactions with the H3 loop (Table 2). Even though Ile^{P675} is responsible for only 6% of the contacts between 4E10 and the peptide, its side chain stacks with the corresponding aliphatic side chains of Ile^{H52} and Ile^{H56} to create a cluster of isoleucines on the edge of the antibody-combining site (Figures 4A and 4C).

Mutagenesis of HIV-1 has recently shown that Trp^{P680} is important for 4E10 neutralization (Zwick et al., 2005). In the peptide studied here, a Lys rather than a Trp was substituted at position 680 to increase peptide solubility. Because this residue is in an α helix, the change from a Lys to a Trp side chain should not affect the helical conformation. However, this change could affect the interactions that this residue makes with the antibody. Thus, to explore the structural role of Trp^{P680} in the binding site, Trp^{P680} was modeled in place of Lys^{P680} in the preferred rotamer that maximizes contacts with 4E10 (Figure 4D). In this conformation, the $N_{\epsilon1}$ atom of Trp^{P680} would hydrogen bond to the carbonyl oxygen of Leu^{H100C}, which corresponds to the hydrogen bond interaction of the N_ξ atom of Lys^{P680} with Leu^{H100C} in the crystal structure. In addition, Trp^{P680} would pack with Tyr^{H32} and Pro^{H100F} (Figure 4D), forming a second cluster of aromatic residues in the antibody-combining site. All of these proposed contacts would place Trp^{P680}, together with Trp^{P672}, Phe^{P673}, Ile^{P675}, and Thr^{P676}, as critical residues for 4E10 specificity.

Discussion

The crystal structure of Fab 4E10, the most broadly neutralizing HIV mAb yet described, was determined as a complex with a 13-residue peptide containing the 4E10 epitope on gp41. The structural analysis of the contributions made by each peptide residue to 4E10 binding reveals the key epitope residues which complement and extend the results obtained from epitope mapping (Zwick et al., 2001a; Stiegler et al., 2001) and mutagenesis experiments (Zwick et al., 2005). Previously, 4E10 was mapped to a linear epitope comprising residues NWF(D/N)IT (Zwick et al., 2001a; Stiegler et al., 2001) on the 671–679 Trp-rich region of gp41. The crystal structure of the Fab 4E10-epitope complex illustrates that Trp^{P672}, Phe^{P673}, Ile^{P675}, and Thr^{P676} make the greatest number of selective contacts with 4E10 (Figure 4 and Table 2), which presumably dictate the high affinity of 4E10 for the epitope. The side chains of Trp^{P672} and Phe^{P673} (and probably Trp^{P680}; a Lys was present at this position in the peptide used here) are buried in the binding site and are involved in aromatic π-stacking interactions. The most important residue for antibody-peptide binding is Trp^{P672}, which alone is responsible for 36% of the total contacts between the Fab and the peptide. In comparison, Ile^{P675} and Thr^{P676} have a secondary role in defining 4E10 specificity. Thr^{P676} can be replaced by a serine without affecting 4E10 binding, and Ser is found in many HIV isolates that are neutralized by 4E10. Such a Thr/Ser change can maintain the hydrogen bond with CDR H3 residue Glu^{H95}. On the other hand, Ile^{P675}, which is highly conserved and forms part of a cluster of three isoleucines in the binding site, is not involved in as many contacts with 4E10 and could perhaps be replaced by other medium-size hydrophobic residues, such as Leu or Val, without any drastic decrease in 4E10 affinity for gp41.

The Fab 4E10-epitope structure demonstrates why 4E10 is very broadly neutralizing. First, the WFXI(T/S) motif, where X does not play a major role in 4E10 binding, appears to be very conserved in all HIV-1 viruses. The absolutely conserved residue Trp^{672} is believed to have a crucial role in virus infectivity (Salzwedel et al., 1999). Second, the somewhat more variable residues that immediately flank the conserved Trp^{P672}, Phe^{P673}, Ile^{P675}, and Thr/Ser^{P676} are located on the opposite side of the helical epitope and are involved in very few contacts with the antibody. These variable residues might be masked in the interface of a gp41 oligomer or embedded in the viral membrane (Figure 5). However, the fact that several HIV isolates with the same 4E10 minimal epitope are differentially neutralized with orders of magnitude difference in potency (Binley et al., 2004) may imply that the 4E10 epitope is not equally exposed on all viruses, with perhaps differences in Env conformation or infection kinetics affecting accessibility to the epitope. Alternatively, other regions of gp41 or even gp120 might also interact with 4E10. The 580 $Å^2$ of surface area buried in the combining site is inside the range typically seen for Fabs binding peptides (usually 400–700 $Å^2$) (Stanfield and Wilson, 1995); however, some available surface in the combining site indicates that residues outside of the core epitope could be involved in binding. This possibility invites further experimental investigation. Furthermore, denaturation of recombinant gp41 reduces the binding of 4E10 but not of 2F5 (Zwick et al., 2001a) and provides further support

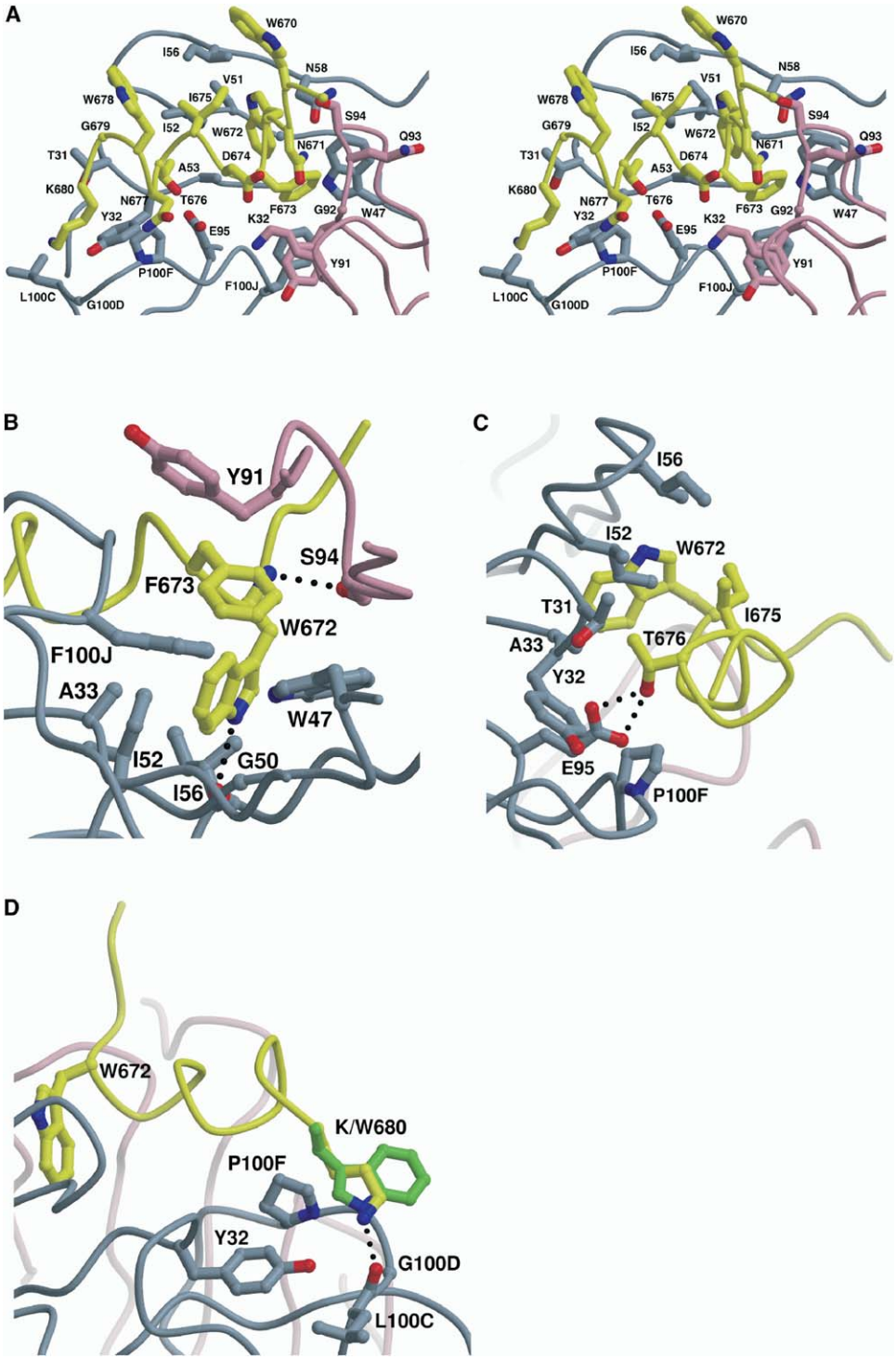

Figure 4. Contacts between Fab 4E10 and Residues of Its Epitope

Hydrogen bonds are shown as dotted lines. Light, heavy, and peptide chains are shown in pink, gray, and yellow, respectively.

(A) Stereo view of the antigen binding site.

(B) Contacts between Fab 4E10 and key peptide residues Trp^{P672} and Phe^{P673}.

(C) Contacts between Fab 4E10 and key peptide residues Ile^{P675} and Thr^{P676}.

(D) Contacts between Fab 4E10 and key peptide residues Lys^{P680} (for solubility) and modeled Trp^{P680} (green) that represents the actual residue in the gp41 sequence. The side chain of Trp^{P672} is shown in (B)–(D) for reference.

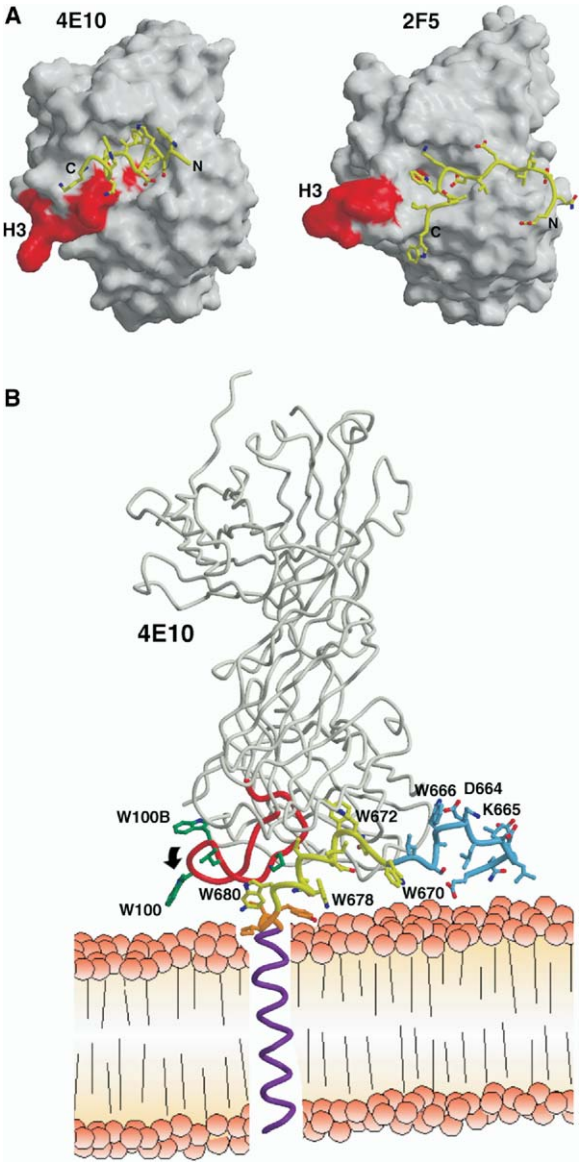

Figure 5. Structural Considerations of Antibody Recognition of the Membrane-Proximal Region of gp41

(A) CDR H3 residues not in contact with antigen are colored in red on the molecular surfaces of 4E10 and 2F5 (PDB entry 1TJI). The equivalent CDR H3 residues colored in red have been seen to contact antigen in a survey of 26 antibody complex structures (MacCallum et al., 1996). This shows that 4E10 and 2F5 might contact additional gp41 or gp120 residues or, more likely, the viral membrane when interacting with intact virus. The peptide is displayed for reference.

(B) Model for the interaction between 4E10 (gray) and its membrane-proximal epitope on gp41. Many constraints are imposed on the 4E10 epitope in the context of the virus, including the proximity of both the viral membrane and the neighboring subunits of the trimeric envelope spike (not shown). The peptide epitope (yellow), the CDR H3 loop (red tube with green side chains), and the modeled Tyr-Ile-Lys residues (orange) that link the peptide epitope region to the modeled gp41 transmembrane domain (purple) are all in close proximity to the surface of the membrane. Certain Trp residues of the peptide, i.e., Trp^{678}, Trp^{680}, and Trp^{670}, could be involved in intimate membrane interactions, e.g., if the 4E10 epitope becomes embedded in the membrane interface with its helical axis parallel to the bilayer. Additionally, some degree of conformational flexibility in the H3 loop may allow Trp^{100} and Trp^{100B} to interact with the membrane. Although, in our structure, Trp^{100} makes a crystal contact that restricts the H3 loop conformational freedom, the tip of the H3 loop would be expected to be flexible in solution. Also modeled is an N-terminal extension of the peptide that includes the adjacent 2F5 epitope using its conformation determined from the crystal structure of the 2F5-peptide complex (PDB entry 1TJI; Ofek et al., 2004). The 2F5 epitope is positioned such that the face recognized by antibody (particularly the DKW core epitope) is pointed away from the viral membrane.

for the importance of the helical epitope conformation for mAb 4E10 binding.

The CDR H3 loop of 4E10, as for 2F5, displays a large surface not involved in antigen contact (Figure 5A). A more typical situation has the CDR H3 in contact with antigen throughout most of its length (MacCallum et al., 1996). This raises the possibility that the CDR H3 loops of 4E10 and 2F5 could make further contacts with the viral membrane (Figure 5B) or with other gp41 or gp120 residues in the context of the intact virus. Additionally, the size, hydrophobic character, and glycine-rich composition of the CDR H3 of 4E10 may be an important feature to facilitate interaction with the membrane-proximal 4E10 epitope. Five Gly and two Trp residues are present among the 18 residues of the H3 loop. The five Gly residues may give the CDR H3 sufficient conformational flexibility to access the membrane surface when bound to the membrane-proximal 4E10 epitope on gp41 (Figure 5B). The H3 loop flexibility would also allow a potential interaction between the central region of the loop (Pro^{H100F}) and Trp^{680}, a gp41 residue located only three residues from the membrane (Figures 4D and 5B). Simultaneously, the two Trp residues located at the hydrophobic tip of the H3 loop (Trp^{H100} and Trp^{H100B}) (Figure 3C) could enhance the interaction between 4E10 and virus by interaction of their side chains with the viral membrane when the base of the H3 loop encounters the gp41 epitope (see e.g., the proposed model in Figure 5B). Biochemical analysis using envelope glycoprotein proteoliposomes suggests that 4E10 and 2F5 binding is enhanced in the presence of a lipid membrane (Ofek et al., 2004). Mutagenesis studies of the H3 loop of 4E10 are ongoing to test the importance of the CDR H3 for 4E10 binding to gp41 on virus particles.

In addition, 4E10 also has an unusually hydrophobic H2 loop that has the most extensive interactions with the peptide epitope (41% of total contacts). The largely hydrophobic nature of these CDR's H2 and H3 makes the 4E10 combining site considerably more hydrophobic (Figure 3D) than those of most antibodies. Thus, elucidation of the critical features of 4E10 recognition of HIV-1 helps to define potential immunogens able to elicit 4E10-like antibodies. For instance, a helical presentation of the core epitope in proximity to a hydrophobic environment, such as a membrane, would appear to be a useful start for design of a vaccine candidate.

Experimental Procedures

Fab 4E10 Preparation, Crystallization, and Data Collection

Recombinant IgG1(κ) 4E10 was overexpressed in Chinese hamster ovary cells as previously described (Buchacher et al., 1994; Kunert

et al., 2000). Antigen binding fragment Fab 4E10 was obtained by papain digestion of IgG1 4E10. Mercuripapain (Sigma; enzyme at 0.5 mg/ml) was preactivated with 10 mM cysteine and 1.25 mM EDTA in 0.1 M sodium acetate (pH 5.5) for 15 min at 37°C. Activated papain solution was then added to IgG1 4E10 (at 5 mg/ml in 0.1 M sodium acetate [pH 5.5]) to give a final w/w ratio of 4% papain, and the reaction was incubated at 37°C for 4 hr. Iodoacetamide (20 mM) was added and followed by further incubation at 37°C for 1 hr to stop the digestion reaction.

Fab 4E10 was purified to >95% homogeneity using sequential affinity, size exclusion, and ionic exchange chromatography. Initially, digested sample was diluted 1:3 with 3.0 M NaCl in 0.1 M Tris-HCl (pH 9.0) and loaded onto a recombinant protein A column (Repligen). The nonbound material was diluted 1:3 with 10 mM sodium phosphate (pH 7.0), 0.15 M NaCl, 10 mM EDTA and loaded onto a recombinant protein G Gammabind Plus column (Amersham Pharmacia). The Fab was eluted using 0.1 M acetic acid (pH 3.0) and immediately neutralized with 1/10 volume of 1.0 M $NaHCO_3$. The eluted fractions were pooled, dialyzed against 0.2 M sodium acetate (pH 5.5), and loaded on a Superdex 75 HR16-60 column (Amersham Pharmacia) equilibrated in 0.2 M sodium acetate (pH 5.5). The gel-filtrated pooled fractions were further purified by cation exchange chromatography on a MonoS HR5-5 column (Amersham Pharmacia) with 20 mM sodium acetate (pH 5.5) and a 0–1.0 M NaCl gradient. Pure Fab 4E10 was dialyzed against 20 mM sodium acetate (pH 5.5) and concentrated to 12 mg/ml using a Millipore Ultrafree-15 centrifuge concentrator (10 kDa molecular weight cut-off).

The peptide was synthesized as previously described (Zwick et al., 2001a) and diluted in water to a concentration of 10 mg/ml. Crystals of Fab 4E10 in complex with the peptide were obtained by cocrystallization after overnight preincubation at 4°C of peptide and Fab 4E10 in a molar ratio of 1:5 (protein:peptide). Crystallization conditions for the complex were initially screened in a nanodrop format (total of 100 nl per drop) using a crystallization robot (Syrrx). Promising crystallization conditions were identified and optimized manually. The best crystals of the complex were grown at 22°C by sitting drop vapor diffusion against 10%–12% (w/v) PEG 8000 in 0.1 M sodium acetate (pH 5.0), 10 mM hexamine cobalt trichloride. Prior to being cooled to cryogenic temperatures, crystals were soaked in a cryoprotectant solution of mother liquor containing 25% (v/v) glycerol. Data were collected on beamline 9-2 at the Stanford Synchrotron Radiation Laboratory (SSRL) using a liquid nitrogen cryostream maintained at 90 K and processed using the HKL package (Otwinowski and Minor, 1997) and the CCP4 suite of programs (CCP4, 1994). Diffraction patterns show the contribution of more than one crystalline lattice; however, it was possible to separate and process the diffraction data from the dominant lattice with good final statistics (Table 1).

Structure Determination and Refinement

The structure of Fab 4E10 as a complex with the 13-residue peptide was determined by molecular replacement using AMoRe (Navaza, 1994) and Fab 48G7 (PDB entry 1HKL) as a probe. The structure was refined in CNS (Brünger et al., 1998) and REFMAC (CCP4, 1994). R_{free} was calculated using the same set of 5% randomly assigned reflections in both programs. Fab heavy and light chains were treated separately as rigid bodies for the initial refinement in CNS. The protein model was then refined using torsion angle simulated annealing at 5000 K. Following these initial stages, the refinement proceeded through cycles of positional, temperature factor, and manual rebuilding in XFIT (McRee, 1999) into σ_A-weighted $2F_o - F_c$ and $F_o - F_c$ electron density omit maps. The maximum likelihood target function, bulk solvent corrections, and anisotropic temperature factor corrections were used for the refinement cycles in CNS. Because the amino acid sequence for the antibody (Kunert et al., 2004) became available only when structural refinement was in the last stages, the 4E10 side chains were initially assigned using information from the Kabat database (Kabat et al., 1991) and the electron density maps. Based on the final electron density and especially due to a possible hydrogen bond interaction, light chain residue 11 was modeled as a Gln in the final structure rather than a Leu, as indicated by the sequence data. Density for the peptide was clear after a few cycles of refinement and manual rebuilding of the starting Fab model. Tight noncrystallographic restraints were used early on in the refinement and released gradually toward the end of the refinement. Water molecules were added automatically using cycles of ARP (CCP4, 1994) for placement and REFMAC with TLS groups for refinement, then verified by manual inspection in XFIT. Stereochemical analysis of the refined structure was performed using PROCHECK (CCP4, 1994). Refinement statistics are summarized in Table 1. One of the molecules of the complex in the asymmetric unit (molecule 2) has higher B values (40.4 $Å^2$) than the other (23.3 $Å^2$) due to fewer crystal packing contacts.

Structural Analysis

Superpositions and root-mean-square deviations (rmsd) calculations were carried out using the INSIGHT II package (Accelrys, Inc., San Diego, CA) for pairs of C_H1, C_L, V_H, and V_L domains. Hydrogen bonds between Fab 4E10 and peptide were identified using HBPLUS (McDonald and Thornton, 1994), and van der Waals contacts were assigned with CONTACSYM (Sheriff et al., 1987). Buried surface areas were calculated using MS (Connolly, 1993) with a 1.7 Å probe radius and standard van der Waals radii (Gelin and Karplus, 1979). The Lys^{P680} to Trp^{P680} change was modeled with XFIT (McRee, 1999). Secondary structure was assigned using PROMOTIF (Hutchinson and Thornton, 1996). Graphics were prepared using XFIT (Figures 2, 3E, 3F, 5B, and 5C), RASTER3D (Merritt and Bacon, 1997) (Figures 2–5), GRASP (Nicholls et al., 1991) (Figures 3D and 5A), and MOLSCRIPT (Kraulis, 1991) (Figures 3A–3D, 4, and 5).

Binding Affinity by ELISA

Enzyme-linked immunosorbent assays (ELISA) were used to determine the apparent binding affinity of the antibody for the peptide and gp41. Microplate wells (Corning) were coated overnight at 4°C with 50 μl of PBS containing peptide (4 μg/ml) or recombinant gp41 (4 μg/ml). The wells were washed twice with PBS containing 0.05% Tween 20 and blocked with 3% BSA for 45 min at 37°C. After a single wash, 4E10 (5 μg/ml) was added to the wells in PBS containing 1% BSA and 0.02% Tween and allowed to incubate at 37°C for 2 hr. The wells were washed four times, goat anti-human IgG $F(ab')_2$ alkaline phosphatase (Pierce) diluted 1:500 in PBS containing 1% BSA was added, and the plate was incubated for 40 min at room temperature. The wells were washed four times and developed by adding 50 μl of alkaline phosphatase substrate prepared by adding one tablet of disodium-ρ-nitrophenyl phosphate (Sigma) to 5 ml of alkaline phosphatase staining buffer (pH 9.8), as specified by the manufacturer. After 30 min, the optical density at 405 nm was read on a microplate reader (Molecular Devices).

Acknowledgments

We thank the staff of the Stanford Synchrotron Radiation Laboratory (Beamline 9-2) for beamline support, X. Dai for valuable help on synchrotron trips, S. Ferguson for excellent technical assistance, P. Kwong and G. Ofek for valuable discussions and sharing unpublished data, and X. Zhu for helpful discussions. This work was supported by NIH grants GM-46192 (I.A.W., R.L.S.) and AI-33292 (D.R.B.), American Foundation for AIDS Research fellowship 106427-34-RFHF (R.M.F.C.), and Elizabeth Glaser Pediatric AIDS Foundation (M.B.Z). The Scripps Research Institute would like to thank the International AIDS Vaccine Initiative (IAVI) for its scientific and development support and financial assistance. This is manuscript no. 16500-MB from The Scripps Research Institute.

Received: August 19, 2004
Revised: December 9, 2004
Accepted: December 15, 2004
Published: February 22, 2005

References

Afonin, P.V., Fokin, A.V., Tsygannik, I.N., Mikhailova, I.Y., Onoprienko, L.V., Mikhaleva, I.I., Ivanov, V.T., Mareeva, T.Y., Nesmeya-

nov, V.A., Li, N., et al. (2001). Crystal structure of an anti-interleukin-2 monoclonal antibody Fab complexed with an antigenic nonapeptide. Protein Sci. *10*, 1514–1521.

Al-Lazikani, B., Lesk, A.M., and Chothia, C. (1997). Standard conformations for the canonical structures of immunoglobulins. J. Mol. Biol. *273*, 927–948.

Binley, J.M., Wrin, T., Korber, B., Zwick, M.B., Wang, M., Chappey, C., Stiegler, G., Kunert, R., Zolla-Pazner, S., Katinger, H., et al. (2004). Comprehensive cross-clade neutralization analysis of a panel of anti-human immunodeficient virus I monoclonal antibodies. J. Virol. *78*, 13232–13252.

Brünger, A.T., Adams, P.D., Clore, G.M., DeLano, W.L., Gross, P., Grosse-Kunstleve, R.W., Jiang, J.-S., Kuszewski, J., Nilges, N., Pannu, N.S., et al. (1998). Crystallography & NMR system: A new software suite for macromolecular structure determination. Acta Crystallogr. D Biol. Crystallogr. *54*, 905–921.

Buchacher, A., Predl, R., Strutzenberger, K., Steinfellner, W., Trkola, A., Purtscher, M., Gruber, G., Tauer, C., Steindl, F., Jungbauder, A., and Katinger, H. (1994). Generation of human monoclonal antibodies against HIV-1 proteins; electrofusion and Epstein-Barr virus transformation for peripheral blood lymphocyte immortalization. AIDS Res. Hum. Retroviruses *10*, 359–369.

Burton, D.R., Desrosiers, R.C., Doms, R.W., Koff, W.C., Kwong, P.D., Moore, J.P., Nabel, G.J., Sodroski, J., Wilson, I.A., and Wyatt, R.T. (2004). HIV vaccine design and the neutralizing antibody problem. Nat. Immunol. *5*, 233–236.

Calarese, D.A., Scanlan, C.N., Zwick, M.B., Deechongkit, S., Mimura, Y., Kunert, R., Stanfield, R.L., Kelly, J.W., Rudd, P.M., Dwek, R.A., et al. (2003). Antibody domain exchange is an immunological solution to carbohydrate cluster recognition. Science *300*, 2065–2071.

Chan, D.C., Fass, D., Berger, J.M., and Kim, P.S. (1997). Core structure of gp41 from the HIV envelope glycoprotein. Cell *89*, 263–273.

CCP4 (Collaborative Computational Project, Number 4)(1994). The CCP4 suite: programs for protein crystallography. Acta Crystallogr. D Biol. Crystallogr. *50*, 760–763.

Connolly, M.L. (1993). The molecular surface package. J. Mol. Graph. *11*, 139–141.

Dimitrov, A.S., Rawat, S.S., Jiang, S., and Blumenthal, R. (2003). Role of the fusion peptide and membrane-proximal domain in HIV-1 envelope glycoprotein-mediated membrane fusion. Biochemistry *42*, 14150–14158.

Ferrantelli, F., and Ruprecht, R.M. (2002). Neutralizing antibodies against HIV - back in the major leagues? Curr. Opin. Immunol. *14*, 495–502.

Gallo, S.A., Finnegan, C.M., Viard, M., Raviv, Y., Dimitrov, A., Rawat, S.S., Puri, A., Durell, S., and Blumenthal, R. (2003). The HIV Env-mediated fusion reaction. Biochim. Biophys. Acta *1614*, 36–50.

Gelin, B.R., and Karplus, M. (1979). Side-chain torsional potentials: effect of dipeptide, protein, and solvent environment. Biochemistry *18*, 1256–1268.

Hutchinson, E.G., and Thornton, J.M. (1996). PROMOTIF-a program to identify and analyze structural motifs in proteins. Protein Sci. *5*, 212–220.

Kabat, E.A., Wu, T.T., Perry, H.M., Gottesman, K.S., and Foeller, C. (1991). Sequences of Proteins of Immunological Interest (Washington, DC: U.S. Department of Health and Human Services).

Kitabwalla, M., Ferrantelli, F., Wang, T., Chalmers, A., Katinger, H., Stiegler, G., Cavacini, L.A., Chou, T.C., and Ruprecht, R.M. (2003). Primary African HIV clade A and D isolates: effective cross-clade neutralization with a quadruple combination of human monoclonal antibodies raised against clade B. AIDS Res. Hum. Retroviruses *19*, 125–131.

Kraulis, P.J. (1991). MOLSCRIPT: a program to produce both detailed and schematic plots of protein structures. J. Appl. Crystallogr. *24*, 946–950.

Kunert, R., Steinfellner, W., Purtscher, M., Assadian, A., and Katinger, H. (2000). Stable recombinant expression of the anti HIV-1 monoclonal antibody 2F5 after IgG3/IgG1 subclass switch in CHO cells. Biotechnol. Bioeng. *67*, 97–103.

Kunert, R., Wolbank, S., Stiegler, G., Weik, R., and Katinger, H. (2004). Characterization of molecular features, antigen-binding, and *in vitro* properties of IgG and IgM variants of 4E10, an anti-HIV type 1 neutralizing monoclonal antibody. AIDS Res. Hum. Retroviruses *20*, 755–762.

Kwong, P.D., Wyatt, R., Robinson, J., Sweet, R.W., Sodroski, J., and Hendrickson, W.A. (1998). Structure of an HIV gp120 envelope glycoprotein in complex with the CD4 receptor and a neutralizing human antibody. Nature *393*, 648–659.

MacCallum, R.M., Martin, A.C.R., and Thornton, J.M. (1996). Antibody-antigen interactions: contact analysis and binding site topography. J. Mol. Biol. *262*, 732–745.

Mascola, J.R. (2003). Defining the protective antibody response for HIV-1. Curr. Mol. Med. *3*, 209–216.

McDonald, I.K., and Thornton, J.M. (1994). Satisfying hydrogen bonding potential in proteins. J. Mol. Biol. *238*, 777–793.

McRee, D.E. (1999). XtalView/Xfit—A versatile program for manipulating atomic coordinates and electron density. J. Struct. Biol. *125*, 156–165.

Merritt, E.A., and Bacon, D.J. (1997). Raster3D: photorealistic molecular graphics. Methods Enzymol. *277*, 505–524.

Munoz-Barroso, I., Salzwedel, K., Hunter, E., and Blumenthal, R. (1999). Role of the membrane-proximal domain in the initial stages of human immunodeficiency virus type 1 envelope glycoprotein-mediated membrane fusion. J. Virol. *73*, 6089–6092.

Muster, T.F., Steindl, F., Purtscher, M., Trkola, A., Klima, A., Himmler, G., Ruker, F., and Katinger, H. (1993). A conserved neutralizing epitope on gp41 of human immunodeficiency virus type 1. J. Virol. *67*, 6642–6647.

Navaza, J. (1994). AMoRe: an automated package for molecular replacement. Acta Crystallogr. A *50*, 157–163.

Nicholls, A., Sharp, K.A., and Honig, B. (1991). Protein folding and association: insights from the interfacial and thermodynamic properties of hydrocarbons. Proteins *11*, 281–296.

Otwinowski, Z., and Minor, W. (1997). Processing of X-ray diffraction data collected in oscillation mode. Methods Enzymol. *276A*, 307–326.

Ofek, G., Tang, M., Sambor, A., Katinger, H., Mascola, J.R., Wyatt, R., and Kwong, P.D. (2004). World Intellectual Property Organization patent WO-00/61618. J. Virol. *78*, 10724–10737.

Pai, E.F., Klein, M.H., Chong, P., and Pedyczak, A. (2000). World Intellectual Property Organization patent WO-00/61618.

Salzwedel, K., West, J.T., and Hunter, E. (1999). A conserved tryptophan-rich motif in the membrane-proximal region of the human immunodeficiency virus type 1 gp41 ectodomain is important for Env-mediated fusion and virus infectivity. J. Virol. *73*, 2469–2480.

Saphire, E.O., Parren, P.W., Pantophlet, R., Zwick, M.B., Morris, G.M., Rudd, P.M., Dwek, R.A., Stanfield, R.L., Burton, D.R., and Wilson, I.A. (2001). Crystal structure of a neutralizing human IgG against HIV-1: a template for vaccine design. Science *293*, 1155–1159.

Schibli, D.J., Montelaro, R.C., and Vogel, H.J. (2001). The membrane-proximal tryptophan-rich region of the HIV glycoprotein, gp41, forms a well-defined helix in dodecylphosphocholine micelles. Biochemistry *40*, 9570–9578.

Sheriff, S., Hendrickson, W.A., and Smith, J.L. (1987). Structure of myohemerythrin in the azidomet state at 1.7/1.3 Å resolution. J. Mol. Biol. *197*, 273–296.

Stanfield, R.L., and Wilson, I.A. (1995). Protein-peptide interactions. Curr. Opin. Struct. Biol. *5*, 103–113.

Stanfield, R., Cabezas, E., Satterthwait, A.C., Stura, E.A., Profy, A.T., and Wilson, I. (1999). Dual conformations for the HIV-1 gp120 V3 loop in complexes with different neutralizing Fabs. Struct. Fold. Des. *7*, 131–142.

Stanfield, R.L., Gorny, M.K., Williams, C., Zolla-Pazner, S., and Wilson, I.A. (2004). Structural rationale for the broad neutralization of

HIV-1 by human monoclonal antibody 447–52D. Structure (Camb.) *12*, 193–204.

Stiegler, G., Kunert, R., Purtscher, M., Wolbank, S., Voglauer, R., Steindl, F., and Katinger, H. (2001). A potent cross-clade neutralizing human monoclonal antibody against a novel epitope on gp41 of human immunodeficiency virus type 1. AIDS Res. Hum. Retroviruses *17*, 1757–1765.

Suarez, T., Gallaher, W.R., Agirre, A., Goni, F.M., and Nieva, J.L. (2000). Membrane interface-interacting sequences within the ectodomain of the human immunodeficiency virus type 1 envelope glycoprotein: putative role during viral fusion. J. Virol. *74*, 8038–8047.

van den Elsen, J.M., Kuntz, D.A., Hoedemaeker, F.J., and Rose, D.R. (1999). Antibody C219 recognizes an alpha-helical epitope on P-glycoprotein. Proc. Natl. Acad. Sci. USA *96*, 13679–13684.

Weissenhorn, W., Dessen, A., Harrison, S.C., Skehel, J.J., and Wiley, D.C. (1997). Atomic structure of the ectodomain from HIV-1 gp41. Nature *387*, 426–430.

Wyatt, R., and Sodroski, J. (1998). The HIV-1 envelope glycoproteins: fusogens, antigens, and immunogens. Science *280*, 1884–1888.

Zwick, M.B., Labrijn, A.F., Wang, M., Spenlehauer, C., Saphire, E.O., Binley, J.M., Moore, J.P., Stiegler, G., Katinger, H., Burton, D.R., and Parren, P.W. (2001a). Broadly neutralizing antibodies targeted to the membrane-proximal external region of human immunodeficiency virus type 1 glycoprotein gp41. J. Virol. *75*, 10892–10905.

Zwick, M.B., Wang, M., Poignard, P., Stiegler, G., Katinger, H., Burton, D.R., and Parren, P.W. (2001b). Neutralization synergy of human immunodeficiency virus type 1 primary isolates by cocktails of broadly neutralizing antibodies. J. Virol. *75*, 12198–12208.

Zwick, M.B., Jensen, R., Church, S., Wang, M., Stiegler, G., Katinger, H., and Burton, D.R. (2005). Anti-human immunodeficiency virus type 1 (HIV-1) antibodies 2F5 and 4E10 require surprisingly few crucial residues in the membrane-proximal external region of glycoprotein gp41 to neutralize HIV-1. J. Virol. *79*, 1252–1261.

Accession Numbers

Coordinates and structure factors for Fab 4E10-peptide have been deposited in the Protein Data Bank under accession code 1TZG.